HHS Public Access

Author manuscript

J Mol Biol. Author manuscript; available in PMC 2023 January 30.

Published in final edited form as:

J Mol Biol. 2022 January 30; 434(2): 167355. doi:10.1016/j.jmb.2021.167355.

Differential activity of APOBEC3F, APOBEC3G, and APOBEC3H in the restriction of HIV-2

Morgan E. Meissner[a], **Nora A. Willkomm**[a], **Jamie Lucas**[a], **William G. Arndt**[a], **Sarah F. Aitken**[a], **Emily J. Julik**[a], **Sunanda Baliga**[a], **Louis M. Mansky**[a,*]

[a]Institute for Molecular Virology, University of Minnesota, 515 Delaware St SE, Moos Tower 18-242, Minneapolis, MN

Abstract

Human immunodeficiency virus (HIV) mutagenesis is driven by a variety of internal and external sources, including the host APOBEC3 (apolipoprotein B mRNA editing enzyme catalytic polypeptide-like 3; A3) family of restriction factors, which catalyze G-to-A transition mutations during virus replication. HIV-2 replication is characterized by a relative lack of G-to-A mutations, suggesting infrequent restriction by A3 proteins. To date, the activity of the A3 repertoire against HIV-2 has remained largely uncharacterized, and the mutagenic activity of these proteins against HIV-2 remains to be elucidated. In this study, we provide the first comprehensive characterization of the restrictive capacity of A3 proteins against HIV-2 in cell culture using a dual fluorescent reporter HIV-2 vector virus. We found that A3F, A3G, and A3H restricted HIV-2 infectivity in the absence of Vif and were associated with significant increases in the frequency of viral mutants. These proteins increased the frequency of G-to-A mutations within the proviruses of infected cells as well. A3G and A3H also reduced HIV-2 infectivity via inhibition of reverse transcription and the accumulation of DNA products during replication. In contrast, A3D, did not exhibit any restrictive activity against HIV-2, even at higher expression levels. Taken together, these results provide evidence that A3F, A3G, and A3H, but not A3D, are capable of HIV-2 restriction. Differences in A3-mediated restriction of HIV-1 and HIV-2 may serve to provide new insights in the observed mutation profiles of these viruses.

*Address correspondence to: Louis M. Mansky, mansky@umn.edu, Phone: (612) 626-5525; fax: (612) 626-5515.

CRediT author statement

Morgan E Meissner: Conceptualization; Methodology; Validation; Resources; Data Curation; Supervision; Writing – Original Draft; Writing - /Review & Editing; Visualization; Funding acquisition

Nora A. Willkomm: Methodology; Validation; Data Curation; Writing – Original Draft; Visualization; Funding acquisition

Jamie Lucas: Data Curation; Visualization

William G. Arndt: Data Curation; Writing - /Review & Editing; Visualization; Funding acquisition

Sarah F. Aitken: Data Curation

Emily J. Julik: Data Curation; Funding acquisition

Sunanda Baliga: Data Curation

Louis M Mansky: Conceptualization; Methodology; Supervision; Project Administration; Conceptualization; Resources; Writing - / Review & Editing; Funding acquisition

Declaration of Interest

None

Graphical Abstract

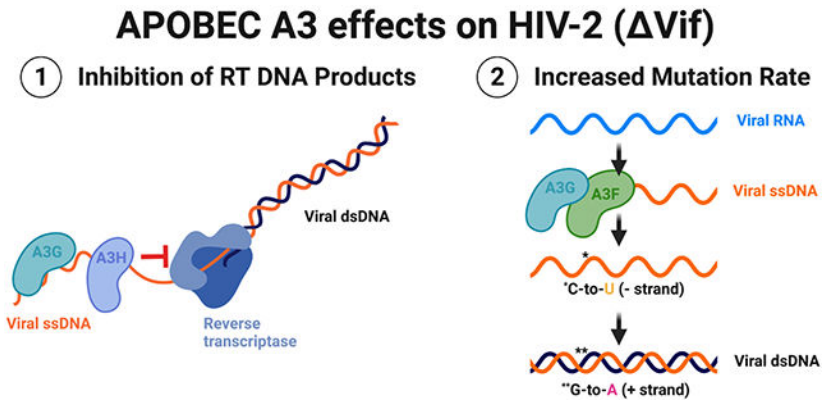

Keywords

retrovirus; cytidine deaminase; mutagenesis; lentivirus; restriction factor

Introduction

An estimated one to two million individuals are infected with human immunodeficiency virus type 2 (HIV-2).[1, 2] Within the context of the global HIV epidemic, HIV-2 exhibits significant geographical constraint, with the majority of infections found in West Africa.[1-3] Progression of HIV-2 infection results in acquired immunodeficiency syndrome (AIDS) if left untreated, which is characterized by significant depletion of CD4+ T cell reservoirs and increased susceptibility to opportunistic infections. HIV-2 exhibits a significantly attenuated disease phenotype compared with HIV type 1 (HIV-1), characterized by lower viral loads within individuals, lower rates of transmissibility between individuals, and a slower progression to AIDS.[4-8] HIV-2 has also been found to exhibit a significantly lower mutation frequency than HIV-1.[9, 10] A high rate of mutation and recombination during HIV replication drives the generation of genetically diverse populations of viruses both between and within hosts, which promotes the emergence of antiviral drug resistance, frustrates vaccine development, and is a key contributor in the persistence of HIV infections on both the individual and global scale.

The error-prone reverse transcriptase (RT) is the primary driver of viral mutagenesis.[11, 12] Host factors can contribute to viral mutagenesis as well, including the APOBEC3 (apolipoprotein B mRNA editing enzyme catalytic polypeptide-like 3; A3) family of cellular factors. The A3 proteins are a family of DNA-editing enzymes, of which a subset (A3D, A3F, A3G, and A3H) have been identified as restriction factors of HIV-1 infection through viral mutagenesis.[13-19] During reverse transcription, these proteins catalyze the deamination of cytosine to uracil in the single-stranded DNA (ssDNA) of the replicating viral genome, templating the improper insertion of an adenine in place of a guanine in the complementary strand. This activity results in the accumulation of G-to-A transition mutations within HIV-1 proviruses, which preferentially occur in a 5’-GG-3’ or 5’-GA-3’ dinucleotide context.[19-21] The HIV viral infectivity factor (Vif) protein

targets A3 proteins for degradation such that restriction of infectivity is circumvented.[19, 22] However, sublethal levels of G-to-A transition mutations are still observed in HIV-1, indicating the incomplete suppression of antiretroviral defense mechanisms.[12, 23]

Studies examining the mutation profile of HIV-2 have observed a relative lack of accumulation of G-to-A mutations within the HIV-2 genome.[9, 10] Compared with HIV-1, G-to-A mutations occur at a frequency approximately 7-fold lower in HIV-2, suggestive of a relative lack of mutagenic activity of A3 proteins against HIV-2.[9, 10] G-to-A mutations associated with A3 restriction have been linked to cell tropism changes,[24] immune evasion,[25, 26] and failure of antiretroviral therapy [27] during HIV-1 infection. A lack of A3-mediated mutagenesis against HIV-2 could therefore explain the low fitness and pathogenicity observed for HIV-2.[9] There is a knowledge gap regarding the understanding of the relationship between A3 proteins and HIV-2. Previous studies on the anti-HIV-2 activity of A3 proteins have been conducted in a piecewise fashion, primarily as an evolutionary comparator with HIV-1 and simian immunodeficiency virus (SIV), and have not included a careful characterization of the mutagenic capacity of these proteins against HIV-2.[28-31]

Given the lack of G-to-A mutations observed during HIV-2 replication, we sought to define the restrictive capacity of the HIV-1-restrictive A3 proteins (A3D, A3F, A3G, and A3H) against HIV-2 and their mutagenic activity against the virus. While we found that A3F, A3G, and A3H were able to restrict HIV-2 infection, A3D had no effect on viral infectivity. Using a dual fluorescent reporter assay, A3F, A3G, and A3H were found to inhibit viral infection and increase the mutant frequency. Proviral sequencing revealed that A3F and A3G have a strong propensity for HIV-2 mutagenesis, and A3G and A3H were found to be potent inhibitors of viral reverse transcription. While A3D is known to inhibit HIV-1 infection, HIV-2 replication was not restricted by A3D. Taken together, these results suggest that HIV-2 infection is restricted by A3F, A3G, and A3H, but not A3D. To our knowledge, this study represents the first comprehensive assessment of the restrict capacity of A3 proteins against HIV-2 infection. The results from this study serve to provide new insights into the differences observed in the mutation frequency and spectra between HIV-1 and HIV-2. Analyses of the interplay between the A3 proteins and HIV-2 replication provides deeper insights into the greater understanding of HIV restriction and mutagenesis.

Results

Comparative analyses of A3 gene expression following HIV-2 infection in a T cell line and primary human T cells.

To determine the effect of HIV-2 infection on *A3D*, *A3F*, *A3G*, and *A3H* expression in T cells, a comparative analysis was done using both a T cell line (*i.e.*, CEM-GFP) as well as primary human CD4+ T cells. First, CEM-GFP T cells were infected with the HIV-2 vector virus, HIV-2 pROD10-MIG. This vector contains a dual fluorescent reporter cassette inserted within the *nef* gene to allow for quantification of infection using flow cytometry. [32] A3 mRNA levels were determined using RT-qPCR at 0, 24, 48, and 72 h post-infection in order to assess the fold change in gene expression. Levels of gene expression were then normalized to the change in *A3* expression observed in uninfected cells after 72 h.

Expression of *A3D*, *A3F*, and *A3H* was detectable in CEM-GFP cells at all time points following infection but was not significantly stimulated over the course of infection (Fig. 1a). Peak *A3D* and *A3F* expression was observed at 48 h post-infection but were not significantly different from levels in uninfected controls. In contrast, *A3G* expression was modestly increased over the course of HIV-2 infection (72 h post-infection; 1.5-fold; $P = 0.002$).

To confirm the physiological relevance of the observations made in CEM-GFP cells, expression of the *A3* genes was also quantified in primary CD4+ T cells isolated from whole blood (Fig. 1b). mRNA levels of *A3D* through *A3H* were quantified using RT-qPCR at 0, 24, 32, and 48 h post-infection in order to determine the timing of *A3* expression within the window of viral assembly. The change in gene expression was normalized to the change in expression observed in mock-infected control cells after 48 h, which accounted for the change in gene expression due to T cell activation alone. Following infection with HIV-2, expression of *A3D* through *A3H* was not significantly stimulated over the course of infection, consistent with limited A3 protein activity during HIV-2 replication.

Vif-mediated degradation of A3 proteins and packaging into HIV-2 particles.

Restriction by A3 proteins requires efficient packaging into viral particles during replication. During assembly of HIV-1, A3D, A3F, A3G, and A3H are recruited into budding particles via interactions with viral and cellular RNAs.[19, 33] Restriction occurs following attachment and entry into target cells, where A3 proteins edit viral DNA during reverse transcription. Therefore, in order to restrict HIV-2 infection, A3 proteins must be packaged into virus particles. The accessory protein Vif, however, counteracts A3-mediated restriction by targeting A3 proteins for degradation, preventing their virologic incorporation.

To assess whether A3D, A3F, A3G, and A3H are incorporated into HIV-2 virions, immunoblotting was used to monitor expression of each of the A3 proteins in viral producer cells and cell-free viral supernatant. HEK293T/17 cells were transiently transfected with either a Vif-proficient (Vif +) or Vif-deficient (Vif −) VSV-G-pseudotyped HIV-2 pROD-10 MIG vector virus plasmid alongside each of the individual HA-tagged *A3* plasmid expression constructs.[13] Viral supernatants from A3-expressing HIV-2 producer cells were collected at 48 h to assess packaging into nascent viral particles. Producer cells were collected and lysed alongside viral lysates to assess congruent A3 expression and packaging efficiency. Relative levels of HA-tagged A3 proteins were quantified by analysis of band intensities using ImageJ software.[34, 35] GAPDH and Gag served as internal cellular and viral controls, respectively.

In HIV-2 producer cells, protein levels of A3F, A3G, and A3H were lower in the presence of Vif than in the absence of Vif (Fig. 2a and Fig. 2b), indicative of Vif-mediated degradation of these A3 proteins. The greatest difference in protein levels between Vif+ and Vif− producer cells was observed with A3H. A3D expression was lower than for other A3 proteins but remained unchanged regardless of Vif expression. Despite variability in their cellular expression levels, A3D, A3F, and A3G were packaged into Vif− viral particles at similar levels (Fig. 2c and Fig. 2d). However, viral lysates from Vif+ producer cells contained low levels of A3F, A3G, and A3H, indicating that HIV-2 Vif prevents

incorporation of these proteins into budding particles. Among these proteins, A3F was packaged at the highest levels, but levels of packaging into Vif+ particles were still approximately one-fourth that of Vif− particles. A3D was packaged into viral particles in both the presence and absence of Vif, and at levels similar to those observed for A3F and A3G Vif− particles. Packaging of A3D was not found to be inhibited by Vif expression.

Analysis of A3 restrictive activity against HIV-2 infection.

Cell culture supernatants from HIV-2-producing 293T/17 cells were collected at 48 h and used to infect U373-MAGI-CXCR4 target cells. HIV-2 vector virus stocks were normalized based upon the amount of viral RNA, measured using RT-qPCR (see Materials and Methods). The volume of virus needed to achieve a multiplicity of infection (MOI) of ~1.0 was determined for Vif+ HIV-2 produced in the presence of the empty *A3* expression vector (control virus). Other viruses were then normalized to the control virus based on RT-qPCR analysis of viral RNA levels. Viral infectivity was assessed at 72 h post-infection based on expression of fluorescent reporter genes using flow cytometry.[32] Infectivity was quantified relative to the control virus.

No significant change in viral infectivity was observed for Vif+ HIV-2 in the presence of any of the A3 proteins (Fig. 3a). The relative infectivity of Vif+ HIV-2 was 92.7%, 98.9%, 95.9%, and 84.1% that of the control virus in the presence of A3D, A3F, A3G, and A3H, respectively. In contrast, the infectivity of Vif− HIV-2 was significantly reduced by A3F, A3G, and A3H. In the absence of Vif, HIV-2 infectivity was reduced to 52.6%, 35.3%, and 46.4% of the relative infectivity of the control virus in the presence of A3F, A3G, and A3H, respectively. Compared with the Vif+ virus, A3F, A3G, and A3H diminished the infectivity of Vif− HIV-2 by 1.88-fold (P <0.01), 2.72-fold (P <0.001), and 1.8-fold (P <0.001), respectively.

A3D, however, did not reduce HIV-2 infectivity, regardless of Vif expression (Fig. 3a). No difference was observed in the rates of infection compared with the control virus in either the Vif+ (92.7%) and Vif− (92.5%) viruses. The capacity of A3D to restrict HIV-2 replication may be related to concentration, though, such that a higher protein-to-virus ratio may be needed to achieve HIV-2 restriction.[13] Vif− virus was produced with increasing plasmid molar ratios of A3D:virus (from 1:20 to 1:5). Virus stocks were normalized to the virus produced at a 1:10 plasmid molar ratio with A3D, and were added at quantities corresponding to that needed to achieve an MOI of ~1.0 in the 1:10 A3D:virus sample. No change in infectivity was observed for HIV-2 across the range of A3D concentrations examined (Fig. 3b). At the highest levels tested, A3D expression was previously shown be associated with a nearly 50% restriction in HIV-1 infectivity,[13] but no significant change was observed herein across titrations with HIV-2.

Several previous studies have found that different haplotypes of A3H that exist in the human population exhibit differential antiviral activity against HIV-1.[17, 36-38] Natural variants of A3D exist in the human population as well, including R97C and R248K mutants, which have been shown to have decreased activity against HIV-1.[39] Despite their reduced anti-HIV-1 activity, these haplotypes are present within 4.6% and 11.6% of individuals of African ancestry, respectively.[39] Of particular interest, both of these mutants were

demonstrated to be sensitive to HIV-2 Vif, which was able to rescue infectivity of HIV-1 from A3D-mediated restriction by 20-40%.[39] Given that these haplotypes are observed frequently in regions where HIV-2 is endemic,[39-41] the activity of these A3D mutants against HIV-2 was examined over increasing A3D concentrations. Vif− HIV-2 was produced using co-transfection with increasing amounts of *A3D*-expressing plasmid DNA (0.5, 2, and 4 μg) and were quantified using RT-qPCR. Virus stocks were normalized to the virus produced along with the empty vector control and were used to infect U373-MAGI-CXCR4 targets cell at an MOI of ~1.0 for the control virus. Rates of infection were normalized to the vector control at a 1:20 A3D:virus ratio. No restriction of HIV-2 infection was observed for wildtype (WT) or either of the mutant A3D proteins across all concentrations of A3D (Fig. 3c). Additionally, Vif− HIV-2 retained 100% or higher relative rates of infectivity compared with the control virus in the presence of A3D R248K at all concentrations. At the highest concentrations of A3D R97C, Vif− HIV-2 infectivity was reduced to 68.4% of the relative infectivity of the control virus, but this was not significantly different from Vif− HIV-2 produced in the presence of the empty control vector (70.8%) at the equivalent DNA ratio. Taken together, these results indicate that while A3F, A3G, and A3H restricted HIV-2 infectivity, HIV-2 infection was not restricted by WT A3D or any of its haplotypes, even at relatively high concentrations of the proteins.

Mutagenesis of HIV-2 by A3 proteins.

A hallmark feature of restriction by A3 proteins is the introduction of G-to-A transition mutations in viral genomes, particularly within the context of G-to-A hypermutation. Although Vif allows the virus to circumvent restriction and establish productive infections, sublethal levels of editing by A3 proteins can still occur,[12, 23] such that G-to-A mutations may be observed in as much as 20% of patient-derived viral sequences.[42-46] Sublethal levels of A3-mediated viral mutagenesis can lead to adaptive evolution of the virus, and thus influence disease progression, therapeutic intervention, and virus evolution.[24-27]

The HIV-2 pROD-10 MIG reporter construct allows for rapid characterization of the mutagenic effects of A3 proteins on HIV-2. Flow cytometry was used as previously described to estimate the frequency of functional infectious mutants in the viral population based on the percent of infected cells expressing a single fluorescent marker (either mCherry or EGFP).[32] Mutant frequency was calculated by dividing the total population of single positive cells ($mCherry^{+}/EGFP^{-}$ + $mCherry^{-}/EGFP^{+}$) by the total infected cell population (100-$mCherry^{-}/EGFP^{-}$). This provided an estimate of the proportion of cells in the infected population harboring a mutant provirus. Vif+ and Vif− viruses produced via co-transfection with the *A3* expression constructs were collected at 48 h and used to infect U373-MAGI-CXCR4 cells following normalization as previously described. At 72 h post-infection, cells underwent flow cytometry to estimate the mutant frequency.

In the absence of A3 protein expression, the frequency of HIV-2 mutants was estimated to be approximately 11% in both the Vif+ and Vif− viruses (Fig. 4a). This baseline mutant frequency remained relatively constant for all Vif+ viruses, ranging from 13.4% to 14.4% in the presence of A3D, A3F, A3G, and A3H. The mutant frequency of the Vif− virus, however, was significantly increased by A3F, A3G, and A3H (P <0.0001 for all). The largest

increase was observed for A3F, which increased the mutant frequency of Vif− HIV-2 by 3.3-fold over the Vif+ virus, such that over 48% of infected cells were infected with a mutant virus. The mutant frequency of Vif− HIV-2 was increased 1.8-fold and 2.5-fold over the Vif+ virus by A3G and A3H, respectively. A3D was not associated with any change in the mutant frequency of Vif− HIV-2. This did not change over increasing protein concentrations (Fig. 3b).

Sequencing was performed to determine whether this increase in mutant frequency was associated with the expected pattern of G-to-A mutations associated with A3-mediated restriction. An ~600-base pair region of *EGFP* in HIV-2 pROD-10 MIG proviruses in infected U373-MAGI-CXCR4 cells was subjected to Sanger sequencing to quantify the frequency and spectra of observed mutations. The *EGFP* region was selected due to the high rate of mutation previously observed in HIV-2.[9] Sequencing of proviral DNA allowed for a more direct estimate of the viral mutation frequency of HIV-2 and the effects of the different A3 proteins over flow cytometry.

Table 1 summarizes the sequencing results. In the control virus, Vif+ HIV-2 was estimated to have a mutation frequency of 9.6 x 10^{-5} mutations per base pair (mut/bp) during a single round of replication (Fig. 4b). In the absence of Vif, this increased to approximately 3.4 x 10^{-4} mut/bp. This increase may be due to low levels of expression of endogenous *A3* genes within 293T/17 cells, which do not restrict infection, despite reports of their contributing to sublethal levels of mutagenesis.[9, 10, 47] This is consistent with an increase in the frequency of G-to-A mutations in the Vif− virus, which were located predominantly within a 5’-GA-3’ dinucleotide context (Fig. 4c and Fig. 4d).

A3D demonstrated a modest but non-statistically significant increase in the mutation frequency of Vif+ (1.88 x 10^{-4} mut/bp) and Vif− HIV-2 (4.68 x 10^{-4} mut/bp) (Fig. 4b). The proportion of G-to-A mutations did not differ significantly between the Vif+ (33.3%) and Vif− (41.2%) viruses, and was similar to the proportion of G-to-A mutations observed in the Vif− virus produced in the presence of the vector control (50%; Fig. 4c). In Vif− proviruses, G-to-A mutations were found at similar rates in 5’-GG-3’ and 5’-GA-3’ dinucleotide pairs, as well as non-APOBEC3-specific 5’-GC-3’ dinucleotide sequences.

A significant increase in mutation frequency was observed in Vif− HIV-2 in the presence of A3F and A3G, which increased the mutation frequency 7-fold and 11-fold over Vif+ HIV-2, respectively (P <0.0001 for both). For both proteins, this increase was associated with a drastic shift in the spectra of mutations observed within provirsus of infected cells. In the absence of Vif, G-to-A transitions accounted for approximately 88% of the observed mutations in HIV-2 proviruses in the presence of A3F, the majority of which were located within a 5’-GA-3’ dinucleotide context (Fig. 4c and Fig. 4d). Similarly, G-to-A mutations accounted for 84% of mutations in the presence of A3G, but were predominantly found within the context of 5’-GG-3’ dinucleotide pairs. A number of hypermutated sequences, defined as those with >1 mutation per 100 base pairs, were observed in the presence of A3F as well, although these were rare in the presence of A3G (Table 1). However, despite the restriction of infectivity and increase in mutants observed with A3H, no change in mutation frequency was detected via Sanger sequencing (Fig. 4b). The mutation frequency

of HIV-2 associated with A3H expression was low regardless of Vif expression and was similar to what was observed in the Vif+ control virus (Table 1). Although they were relatively infrequent, G-to-A transitions accounted for the majority (66.7%) of the mutations observed in Vif− HIV-2 in the presence of A3H. Taken together, these results suggest that A3F and A3G are potent mutagens of HIV-2. A3H was not found to significantly increase the mutation frequency of HIV-2, though it could alter the frequency of functional mutants in the population by creating a shift towards G-to-A mutations. Collectively, these results suggest that while A3F and A3G potent mutagens of HIV-2, A3H is not a major source of mutagenesis of HIV-2.

Inhibition of reverse transcription by A3 proteins.

In addition to the mutagenesis of viral DNA, A3G also restricts HIV-1 replication by inhibition of reverse transcription.[48] This occurs when the protein binds ssDNA and RNA with high affinity and sterically hinders RT, resulting in decreased synthesis of viral DNA products.[49-52] Given the observed differences in the mutagenic profiles of A3F, A3G, and A3H, the restriction of HIV-2 infectivity was investigated to determine whether it was related to inhibition of reverse transcription by A3 proteins. Vif+ and Vif− HIV-2 were used to infect U373-MAGI-CXCR4 cells, which were collected at 0, 4, 8, and 24 h post-infection. Cells were lysed for efficient collection of reverse transcription products. Quantitative PCR (qPCR) was used to measure the accumulation of early (minus-strand strong stop) and late (U5-5'UTR) reverse transcription DNA products in cell lysates. Quantities were normalized to the amount of DNA measured at 24 h post-infection for the Vif+ virus produced in the presence of the respective A3 protein.

At both early and late stages of reverse transcription, there was no difference in the accumulation of DNA products associated with A3D expression in the presence or absence of Vif at any point over the course of replication, consistent with previous infection results (Fig. 5a). At 24 h, A3F was associated with a small but nonsignificant decrease in the accumulation of early DNA products (Fig. 5b). This trend was more pronounced for late DNA products, but did not reach statistical significance. A similar trend was observed at 8 h post-infection for late DNA products as well. A small but nonsignificant decrease in early DNA products was also observed at 8 and 24 h for A3G (Fig. 5c) and A3H (Fig. 5d). However, for both A3G and A3H, the accumulation of late DNA products was significantly reduced at 24 h by approximately 80% and 75%, respectively ($P < 0.01$ for both), during Vif− HIV-2 replication. Notably, A3H almost completely inhibited the accumulation of late DNA products in Vif− HIV-2 at 8 h post-infection.

Table 2 provides a summary of the observed anti-HIV-2 activities of A3D, A3F, A3G, and A3H. A3F, A3G, and A3H were all able to restrict HIV-2 infection via differential mechanisms. A3F and A3G were found to exhibit the canonical mutagenic properties typically associated with A3-mediated restriction and were associated with significant increases in both functional mutants in the population and G-to-A mutations within proviral sequences. In contrast, A3H did not significantly increase the mutation frequency of HIV-2, despite increasing the proportion of functional mutants in the population. A shift was observed in the spectra of mutations observed in HIV-2 proviral sequences, indicating

low levels of A3H-driven HIV-2 mutagenesis may still occur. Robust reductions in the accumulation of DNA products during reverse transcription, particularly in the late stages of replication, appear to be the primary mode of HIV-2 restriction mediated by A3H, which was also observed with A3G expression. While A3D is known to act as a restriction factor of HIV-1, no antiretroviral activity was observed with HIV-2.

Discussion

While a high mutation rate is a key driver of HIV-1 evolution and persistence, the mechanisms of HIV-2 mutagenesis remain poorly characterized. Recent studies reveal that HIV-2 is characterized by a relative lack of G-to-A transition mutations, and particularly hypermutations, which are the hallmark signature of DNA editing by APOBEC3 proteins.[9, 10] The lack of G-to-A mutations observed during HIV-2 replication suggests a general lack of restriction of HIV-2 by A3 proteins. However, while the interactions between HIV-1 and A3 proteins have been extensively characterized,[14, 16-18, 22, 24, 27, 37, 53-55] the mutagenic capacity of the A3 repertoire against HIV-2 remains largely uncharacterized and represents an important knowledge gap within the field. To investigate this, a comprehensive examination of the activity of the canonically restrictive A3 proteins against HIV-2 was conducted.

In both a T cell line and primary CD4+ T cells, induction of *A3* expression was not significantly stimulated following HIV-2 infection. The CEM-GFP T cell line is derived from the parental CEM line, which has been previously shown to express all of the *APOBEC3* genes except for *A3A*.[56] As expected, expression of *A3D*, *A3F*, *A3G*, and *A3H* was detectable in CEM-GFP cells at all time points following infection, however a modest but significant change in expression was observed only for *A3G* at 72 h post-infection. Previous studies have indicated that the majority of HIV-1 replication occurs within the first 48 h of infection.[57] The replication kinetics of HIV-1 and HIV-2 do not differ significantly,[10] suggesting that the completion of reverse transcription, provirus formation, and particle release are already established prior to 72 h. Because A3-mediated restriction is thought to be a producer cell-dependent effect, A3 proteins must be present prior to viral particle release in order to observe virus restriction, therefore later expression of *A3* genes may be less relevant for restriction of viral infection.

By transient transfection with *A3* expression constructs, we observed that the A3D, A3F, A3G, and A3H proteins were packaged into virus particles released from Vif− HIV-2 producer cells, but that the packaging of A3F, A3G, and A3H was inhibited in released Vif+ HIV-2 particles. These results indicate that HIV-2 Vif targets A3F, A3G, and A3H for degradation in virus-producing cells, effectively preventing their incorporation into budding particles during virus particle assembly. As expected, incorporation of A3F, A3G, and A3H into Vif− HIV-2 particles was associated with a significant reduction of viral infectivity. While Vif expression maintains HIV-2 infectivity at levels similar to those observed in the absence of A3 expression, Vif− HIV-2 infectivity was reduced by 47%, 65%, and 54% by A3F, A3G, and A3H, respectively. Similar reductions in HIV-1 infectivity have been reported by these A3 proteins at equivalent concentrations.[13]

Restriction of HIV-2 infectivity by A3F, A3G, and A3H was concomitant with significant increases in the proportion of mutants in the viral populations observed using flow cytometry of infected target cells. Interestingly, sequencing of proviruses revealed a more complex association between virus restriction and mutagenesis. A3F, A3G, and A3H protein expression was found to be associated with substantial shifts in the proportion of G-to-A transition mutations in the absence of Vif, but only A3F and A3G were associated with a significant increase in the mutation frequency. The results of these assays are not necessarily incongruent, as different functional outcomes of viral mutagenesis were assessed by each. The use of flow cytometry to detect the expression of fluorescent reporter genes in the HIV-2 vector virus allows for a more high-throughput estimation of functional mutants in the population of infected cells, or the proportion of vector proviruses in which gene expression has been extinguished by mutation(s). The mutations that extinguish fluorescent protein detection may occur in either of the fluorescent reporter genes (*mCherry* or *EGFP*), and/or the internal ribosomal entry site (IRES) that controls *EGFP* gene expression. Nucleotide sequencing provides a more quantitative estimation of the frequency and spectra of mutations introduced into the virus but is limited to the selected amplicon (*i.e.*, *EGFP*). Because A3-mediated mutagenesis is dependent upon both the sequence and secondary structure of the target minus-strand DNA,[21] differences in the frequency of viral mutagenesis may occur between different regions of the genome. Furthermore, the 5’-GG-3’ and 5’-GA-3’ dinucleotide preference of A3 proteins means that G-to-A transition mutations caused by A3-mediated mutagenesis may preferentially introduce nonsense mutations. The shifting of the mutation spectra of Vif− HIV-2 in such a manner that G-to-A transitions represent the dominant mutation observed may therefore increase the frequency of phenotypic mutants in the population without significantly increasing the mutation frequency.

The mutation frequency associated with A3H expression was not significantly different from Vif+ HIV-2 produced in the absence of any A3 proteins, regardless of Vif expression. However, A3H significantly inhibited the accumulation of late DNA products in HIV-2 replication, suggesting that A3H may exert antiviral activity against HIV-2 by viral DNA synthesis blocakde rather than through mutagenesis. As a result, virus restriction by A3H would not result in provirus formation, and those proviruses that do escape A3H restriction would exhibit low levels of mutation. Furthermore, the exclusion of hypermutants from sequence analysis may artificially attenuate the effects of A3 protein expression on the HIV-2 mutation frequency. Hypermutants, which were defined as sequences in which >1 mutation occurred per 100 bases sequenced, were identified in 3 Vif+ and 2 Vif− HIV-2 proviruses formed in experiments in which virus particles were produced in the presence of A3F expression, and in 1 Vif− HIV-2 provirus from viruses produced in the presence of A3G (Table 1). The relative infrequency of G-to-A hypermutants is consistent with previous results for HIV-2, but is in stark contrast to the well-established A3G-associated hypermutation profile observed in HIV-1.[9, 10, 19] Although the exact mechanisms underlying the differences in the mutagenic activity of these proteins, and particularly A3G, remain to elucidated, it is possible that viral RNA and DNA secondary structures may play a role.[21]

A limitation of this research, however, is the inability to make effective comparisons aimed at uncovering the physiological mechanisms that underlie the differences in A3-mediated restriction and mutagenesis of HIV-1 and HIV-2. A clear demonstration of this can be seen when examining the antiretroviral activity of A3D. We observed that HIV-2 infectivity was unaffected by A3D expression, even in the absence of Vif and at increasing protein concentrations, which is consistent with results that have been previously observed with other strains of HIV-2.[31] Furthermore, A3D expression did not affect the mutation frequency of HIV-2, including G-to-A transition mutations characteristic of A3-mediated mutagenesis (Fig. 4). This is in clear contrast to what we observed with HIV-1, in which A3D expression was associated with a significant reduction in viral infectivity as well as an increase in the viral mutation frequency (Fig. 6a and 6b). However, discordant results were observed in the presence of A3D expression when comparing viral mutation spectra associated with Vif-deficient HIV-2 (Fig. 5c), which were characterized by a higher proportion of G-to-A mutations relative to those of Vif-deficient HIV-1 (Fig. 6c). These observations highlight the complexities associated with comparative analyses that examine the restrictive and mutagenic activities of A3 proteins in cell culture.

Taken together, these results indicate that A3F, A3G, and A3H, but not A3D, restrict HIV-2 infectivity. The lack of observed A3D-mediated mutagenesis, together with a propensity for A3H to block HIV-2 reverse transcription rather than mutagenize the virus, helps to provide an explanation for the relative lack of G-to-A transition mutations observed during HIV-2 replication.[9, 10] However, the restrictive activity of A3 proteins is based on a variety of factors, including the efficiency of Vif-mediated degradation, efficiency of packaging, individual A3 mutagenic capacity, and ability to block DNA replication. Parallel, comparative studies of individual A3 proteins and their antiviral activity against HIV-1 and HIV-2 are needed to more exhaustively quantitate the differences in A3-mediated mutagenesis and restriction between these viruses. Such a quantitative analysis of viral mutagenesis will provide a deeper understanding of the differences in the interplay of the A3 proteins with HIV-1 and HIV-2 replication and enhance our current understanding of HIV restriction and mutagenesis.

Materials and Methods

Plasmids, cell lines, and reagents.

The HIV-1 MIG vector and the HIV-2 pROD-10 MIG vector have been previously described.[58, 59] An expression cassette encoding *mCherry* followed by an IRES controlling expression of enhanced green fluorescent protein (*EGFP*) was inserted within the *nef* region of either the HIV-1 genome or the HIV-2 genome, respectively. The vector expresses both *mCherry* and *EGFP*, as well as all viral genes except *nef* and *env*. The Vif− vectors were generated by introduction of two stop codon mutations (*i.e.*, K27stop, Y28stop) within the N-terminus of Vif via site-directed mutagenesis. The HA-tagged *A3* expression constructs have been previously described and were a kind gift from Dr. Reuben Harris (University of Minnesota, Minneapolis, MN).[13]

U373-MAGI-CXCR4 cells were obtained from Dr. Michael Emerman and Dr. Adam Geballe through the NIH AIDS Reagent Program, Division of AIDS, NIAID, NIH.[60,

61] HEK293T/17 (ATCC CRL-11268) and U373-MAGI-CXCR4 cells were cultured in complete Dulbecco's modified Eagle medium (DMEM) from Cellgro supplemented with 10% HyClone FetalClone III (FC3; Thermo Scientific, Waltham, MA) and 1% penicillin-streptomycin (Life Technologies, Carlsbad, CA). CEM-GFP cells, obtained through the NIH AIDS Reagent Program, Division of AIDS, NIAID, NIH from Dr. Jacques Corbeil,[62] were cultured in RPMI (Invitrogen, Carlsbad, CA) supplemented with 10% FC3 and 1% penicillin-streptomycin. Human primary CD4+ T cells were isolated from whole blood obtained from 3 individual blood donors (Memorial Blood Center, Minneapolis, MN) using negative immunomagnetic separation (MACSxpress Whole Blood CD4 T Cell Isolation Kit, Miltenyi). Cells were maintained in RPMI supplemented with 10% FC3, 1% penicillin-streptomycin, and 20 U/mL interleukin (IL)-2 at a density of approximately 2.5 x 10^6 cells/mL.

Virus production, titration, and quantification.

Infectious vector virus was produced in HEK293T/17 cells via co-transfection of virus vector, an HA-tagged *A3* expression construct or empty vector control, and the vesicular stomatitis virus G (*VSVG*) glycoprotein expression vector at a 10:1:1 ratio and 5 μg total DNA, unless otherwise indicated, using GenJet version II (SignaGen, Frederick, MD) in 10 cm plates according to manufacturer's protocols. Media was not replaced at 24 h, but was supplemented with 2 mL complete medium. Supernatant was collected at 48 h, filtered through a 0.2 μm filter, and treated with 1 U DNaseI (New England Biolabs, Ipswich, MA) per μg of DNA at 37°C. Viral stocks were maintained at −80°C. Prior to experimental infections, viral stocks were first titered in the appropriate cell line (CEM-GFP or U373-MAGI-CXCR4). For infections in U373-MAGI-CXCR4 cells, cells were plated the day prior to infection at a density of 31,250 cells per well in a 24-well plate. After 24 h, media was replaced and virus was added over a range of 6.25 to 100 μL by twofold dilution series. Media was replaced at 24 h post-infection. At 72 h post-infection, cells were collected for analysis of infection rates as previously described.[9] Infection was quantified based upon expression of one or both fluorescent reporter proteins (*i.e.*, mCherry and EGFP), as determined using a BD LSR II flow cytometer (BD Biosciences, Franklin Lakes, NJ). EGFP was excited using a blue 488-nm laser and emission detected using the 505LP and 525/50 filters; mCherry was excited using a yellow-green 561 nm laser, with emission detected using the 595LP and 610/20 filters. Virus titration was performed similarly in CEM-GFP cells, with cells plated at a concentration of 80,000 cells per well in 96-well plates at the time of infection.

DNaseI-treated viral stocks were used for vector virus quantification. Viral RNA was extracted in duplicate using the Roche High Pure Viral RNA kit according to manufacturer's protocols and eluted in 50 μL elution buffer. Immediately following extraction, 6 μL of viral RNA was used for cDNA synthesis using the iScript cDNA Synthesis kit (Bio-Rad) and the provided random primers according to manufacturer's instructions. Viral RNA was stored at −80°C and viral cDNA was stored at −20°C for later use. The iTaq Universal SYBR Green Supermix (Bio-Rad, Hercules, CA) was used for qPCR quantification of viral cDNA. The reaction was performed according to manufacturer's protocol in a total volume of 12.5 μL using 1 μL of cDNA synthesis-product as template in duplicate, such that each virus was

quantified in quadruplicate. The HIV-2 RT-qPCR Gag-F (5'- CAG GAT TTC AGG CAC TCT CAG A-3') and HIV-2 RT-qPCR Gag-R (5'- TGC TTG ATG GTC GCC CAC A-3') primers were used for quantification of viral cDNA using an approximately 80-bp region within the *gag* open reading frame. The results from qPCR were used to normalize the quantities used for infection relative to the amount of control virus needed to achieve the desired MOI. HIV-1 quantification was performed in a similar manner with the HIV-1-RT-qPCR Gag-F (5'-CAT GTT TTC AGC ATT ATC AGA AGG A-3') and HIV-1-RT-qPCR Gag-R (5'-TGC TTG ATG TCC CCC CAC T-3') primers for cDNA quantification.

RT-qPCR of A3 mRNA expression in a T cell line and primary human T cells.

Cellular RNA was extracted from infected CEM-GFP cells using the RNeasy Plus Mini kit (Qiagen, Germantown, MD) according to manufacturer's protocol at indicated time points post-infection. The synthesis of cDNA was performed as described above in a total volume of 160 μL using the provided oligo dT primers. Subsequent qPCR reactions were performed in duplicate as described above in a total volume of 10 μL using previously described primers for *A3D*, *A3F*, *A3G*, and *A3H*.[56] The fold change in *A3* gene expression was calculated relative to the expression at time zero. Infections and analyses of expression were performed in triplicate, and the mean and standard deviation of results are reported. Significance was determined using unpaired t-tests and corrected for multiple hypothesis testing.

Primary human CD4+ T cells were seeded at a density of 2.5 x 10^6 cells/mL in RPMI with FC3 and penicillin-streptomycin. Cells were treated with 20 U/mL IL-2 and 1X phytohemagglutinin-L for stimulation; untreated cells served as an unstimulated control. After incubation for 72 h, cells were seeded in a 96-well plate at 80,000 cells per well. Cells were pelleted (1500 x *g*, 2 min) and their medium removed and replaced with an inoculum of HIV-2 virus-containing supernatants diluted in a total volume of 100 μL complete medium. For mock infections, 100 μL complete medium alone was used. Cells were spinoculated for 2 h at 1200 x *g* at room temperature, after which the inoculum was immediately replaced with complete medium. Samples were collected by pooling the contents of 3 wells at 0, 24, 32, and 48 h post-infection. The contents of the pooled wells were pelleted at 4300 x *g* for 5 min, the supernatants aspirated, and the cell pellets flash frozen for subsequent RNA extraction. RNA was extracted using the RNeasy kit and converted to cDNA using the iScript Select kit. Infections and analyses of expression were performed in triplicate, and the mean and standard deviation of results are reported. Significance was determined using unpaired t-tests and corrected for multiple hypothesis testing.

Immunoblot of HA-tagged A3 proteins.

At 48 h post-transfection as described above, cells and viral supernatant were collected. Supernatant was filtered through a 0.2 μm filter and concentrated at 20,000 x *g* for 60 min. Viral pellets were resuspended in 200 uL of phosphate-buffered saline (PBS) and centrifuged at 20,000 x *g* for an additional 60 min. Viral pellets were resuspended in radioimmunoprecipitation assay (RIPA) buffer (1% IGEPAL CA-630, 50 mM Tris-HCL [pH 7.5], 150 mM NaCl, 0.5% deoxycholate [DOC], 5 mM EDTA, 0.1% sodium dodecyl

sulfate [SDS]) supplemented with a protease inhibitor cocktail (Sigma-Aldrich, Darmstadt, Germany). Cells were washed with PBS and lysed with RIPA buffer with 1X protease inhibitor cocktail and lysates were clarified via centrifugation at 10,000 x *g* for 20 min to obtain the soluble fraction. The total protein content of cell and viral lysates was assessed by using a bicinchoninic acid (BCA) assay (Thermo Scientific), and 20 μg total protein from cell lysate and 8 μg total protein from viral lysate was incubated at room temperature for 60 min with RNAseA (Sigma-Aldrich) at a final concentration of 100 μg/mL. Before loading, samples were boiled in 2X SDS Sample Buffer (100 mM Tris-CL [pH 6.8], 7.5% sodium dodecyl sulfate [SDS], 0.2% bromophenol blue, 20% glycerol, 5 mM dithiothreitol [DTT], 5% 2-mercaptoethanol) at 95 C for 10 min. Cell and viral lysates were subjected to electrophoresis on an SDS-PAGE 4 to 20% gel (GenScript) and transferred to a nitrocellulose membrane (Bio-Rad). HA-tagged A3 was detected with mouse monoclonal anti-HA antibody diluted 1:1000 in Tris-Buffered Saline + Tween (TBS-T) buffer (20 mM Tris, 150mM Nacl, 0.1% Tween 20, [pH 7.5]). HIV-2 was detected with 1:10,000 rabbit polyclonal anti-p24 antibody (AIDS Reagent Program, Division of AIDS, NIAID, NIH: ARP-4250, contributed by DAIDS/NIAID; produced by BioMolecular Technologies), which cross-reacts with both HIV-1 and HIV-2 Gag. GAPDH was detected with 1:1000 rhodamine conjugated anti-GAPDH Fab (Bio-Rad). Membranes were washed before incubation with 1:1000 anti-mouse StarBright B700 (Bio-Rad) and 1:15,000 horseradish peroxidase (HRP)-conjugated goat anti-rabbit (Bio-Rad) antibodies. Protein expression was detected with a ChemiDoc Touch system (Bio-Rad) and analyzed using ImageJ software.[34, 35] Relative levels of HA-tagged A3 proteins were determined by analysis of band intensities. Immunoblotting was performed in experimental triplicate and a representative image was chosen.

HIV infectivity and mutant frequency assay.

Infectivity and mutant rates were estimated using flow cytometry as previously described.[32] Viral infection quantities were normalized using RT-qPCR as described above. Infection rates were normalized to the Vif+ virus produced in the presence of the vector control, which was set to 100%. Differences between Vif+ and Vif− HIV-2 infectivity rates were evaluated for significance using multiple t-tests and corrected for multiple hypothesis testing. Mutant frequency was estimated by calculating the proportion of single-positive cells out of all infected cells [($mCherry^+/EGFP^-$ + $mCherry^-/EGFP^+$)/(100-$mCherry^-/EGFP^-$)]. Significant differences in the mutant frequency of Vif+ and Vif− viruses were determined using multiple t-tests and corrected for multiple hypothesis testing. HIV-1 infectivity and mutant frequency analyses were performed in a similar manner.

Proviral DNA sequence analysis.

Approximately 200,000 target cells from each virus/A3 pair were collected for genomic DNA isolation using the Roche High Pure PCR Template Preparation kit 72 h after infection. An ~600-bp region of *EGFP* was amplified by PCR (*EGFP* For-Primer: 5-GAC GTA AAC GGC CAC AAG TTC-3’; *EGFP* Rev-Primer: 5’-GAA CTC CAG CAG GAC CAT GTG-3’) using the high-fidelity Pfu DNA polymerase (Agilent Technologies). PCR clean-up was performed using the Wizard SV Gel and PCR Clean-Up System (Promega, Madison, WI). PCR products were A-tailed using Taq DNA polymerase (New England

Biolabs) and ligated into the pGEM-T Easy vector (Promega). Plasmids were transformed into DH5α *E. coli* and screened for insertion according to manufacturer's protocols. Plasmid DNA was purified from insert-containing colonies (Monarch Plasmid Miniprep kit, New England Biolabs) and submitted for sequencing (Functional Biosciences, Madison, WI). Sequenced alignment was performed using Lasergene software from DNASTAR.

qPCR analysis of DNA product accumulation.

Approximately 31,250 U373-MAGI-CXCR4 cells were infected with normalized quantities of virus at an MOI of approximately 0.4. Cells were collected at 0, 4, 8, and 24 h post-infection and lysed as previously described.[63] Viral DNA products were quantified using qPCR as described above using primers for early (strong stop DNA; ssDNA For: 5'-CAA GTT AAG TGT GTG CTC CC-3'; ssDNA Rev: 5'-ACC AGG GTC TTG TTA CTC AG-3') and late (late RT; LRT For: 5'-CCT GGT CAT TCG GTG TTC A-3'; LRT Rev: 5'-AGC CGT GTT CCA AGA CTT C-3') reverse transcription products. Products were normalized to 18S DNA (18S For: 5'-GTA ACC CGT TGA ACC CCA TT-3'; 18S Rev: 5'-CCA TCC AAT CGG TAG TAG CG-3'). Changes in gene expression were evaluated using the $2^{-\Delta\Delta CT}$ method and were normalized between experiments using an uninfected control. Infections were performed in triplicate and analyzed for statistical significance using multiple t-tests across time points, with correction for multiple hypothesis testing.

Acknowledgements

This work was supported by National Institutes of Health grant R01 AI150468 (to L.M.M.). M.E.M. was supported by NIH grants T32 AI083196 and F31 AI 50487; E.J. was supported by NIH grant T32 HL007741. N.A.W. was supported by NIH grant F30 DE031829; W.G.A. was supported by NIH grant T32 AI083196. We thank Jonathan O. Rawson, for his guidance and expert feedback; Nathaniel Talledge, for his artistic support and keen eye for design; and Sofia Nóbrega de Moraes, for her assistance in troubleshooting immunoblot experiments.

References

[1]. Visseaux B, Damond F, Matheron S, Descamps D, Charpentier C. Hiv-2 molecular epidemiology. Infect Genet Evol. 2016;46:233–40. [PubMed: 27530215]

[2]. Gottlieb GS, Raugi DN, Smith RA. 90-90-90 for HIV-2? Ending the HIV-2 epidemic by enhancing care and clinical management of patients infected with HIV-2. Lancet HIV. 2018;5:e390–e9. [PubMed: 30052509]

[3]. Nicolas D, Ambrosioni J, Paredes R, Marcos MA, Manzardo C, Moreno A, et al. Infection with human retroviruses other than HIV-1: HIV-2, HTLV-1, HTLV-2, HTLV-3 and HTLV-4. Expert Rev Anti Infect Ther. 2015;13:947–63. [PubMed: 26112187]

[4]. Kanki PJ, Travers KU, S MB, Hsieh CC, Marlink RG, Gueye NA, et al. Slower heterosexual spread of HIV-2 than HIV-1. Lancet. 1994;343:943–6. [PubMed: 7909009]

[5]. Adjorlolo-Johnson G, De Cock KM, Ekpini E, Vetter KM, Sibailly T, Brattegaard K, et al. Prospective comparison of mother-to-child transmission of HIV-1 and HIV-2 in Abidjan, Ivory Coast. JAMA. 1994;272:462–6. [PubMed: 8040982]

[6]. Popper SJ, Sarr AD, Travers KU, Guèye-Ndiaye A, Mboup S, Essex ME, et al. Lower human immunodeficiency virus (HIV) type 2 viral load reflects the difference in pathogenicity of HIV-1 and HIV-2. J Infect Dis. 1999;180:1116–21. [PubMed: 10479138]

[7]. O'Donovan D, Ariyoshi K, Milligan P, Ota M, Yamuah L, Sarge-Njie R, et al. Maternal plasma viral RNA levels determine marked differences in mother-to-child transmission rates of HIV-1 and HIV-2 in The Gambia. MRC/Gambia Government/University College London Medical School working group on mother-child transmission of HIV. AIDS. 2000;14:441–8. [PubMed: 10770548]

[8]. Marlink R, Kanki P, Thior I, Travers K, Eisen G, Siby T, et al. Reduced rate of disease development after HIV-2 infection as compared to HIV-1. Science. 1994;265:1587–90. [PubMed: 7915856]

[9]. Rawson JM, Landman SR, Reilly CS, Mansky LM. HIV-1 and HIV-2 exhibit similar mutation frequencies and spectra in the absence of G-to-A hypermutation. Retrovirology. 2015;12:60. [PubMed: 26160407]

[10]. Rawson JMO, Gohl DM, Landman SR, Roth ME, Meissner ME, Peterson TS, et al. Single-Strand Consensus Sequencing Reveals that HIV Type but not Subtype Significantly Impacts Viral Mutation Frequencies and Spectra. J Mol Biol. 2017.

[11]. Menendez-Arias L Mutation rates and intrinsic fidelity of retroviral reverse transcriptases. Viruses. 2009;1:1137–65. [PubMed: 21994586]

[12]. Delviks-Frankenberry KA, Nikolaitchik OA, Burdick RC, Gorelick RJ, Keele BF, Hu WS, et al. Minimal Contribution of APOBEC3-Induced G-to-A Hypermutation to HIV-1 Recombination and Genetic Variation. PLoS Pathog. 2016;12:e1005646. [PubMed: 27186986]

[13]. Hultquist JF, Lengyel JA, Refsland EW, LaRue RS, Lackey L, Brown WL, et al. Human and rhesus APOBEC3D, APOBEC3F, APOBEC3G, and APOBEC3H demonstrate a conserved capacity to restrict Vif-deficient HIV-1. J Virol. 2011;85:11220–34. [PubMed: 21835787]

[14]. Chaipan C, Smith JL, Hu WS, Pathak VK. APOBEC3G restricts HIV-1 to a greater extent than APOBEC3F and APOBEC3DE in human primary CD4+ T cells and macrophages. J Virol. 2013;87:444–53. [PubMed: 23097438]

[15]. Ooms M, Brayton B, Letko M, Maio SM, Pilcher CD, Hecht FM, et al. HIV-1 Vif adaptation to human APOBEC3H haplotypes. Cell Host Microbe. 2013;14:411–21. [PubMed: 24139399]

[16]. Sato K, Takeuchi JS, Misawa N, Izumi T, Kobayashi T, Kimura Y, et al. APOBEC3D and APOBEC3F potently promote HIV-1 diversification and evolution in humanized mouse model. PLoS Pathog. 2014;10:e1004453. [PubMed: 25330146]

[17]. Refsland EW, Hultquist JF, Luengas EM, Ikeda T, Shaban NM, Law EK, et al. Natural polymorphisms in human APOBEC3H and HIV-1 Vif combine in primary T lymphocytes to affect viral G-to-A mutation levels and infectivity. PLoS Genet. 2014;10:e1004761. [PubMed: 25411794]

[18]. Krisko JF, Begum N, Baker CE, Foster JL, Garcia JV. APOBEC3G and APOBEC3F Act in Concert To Extinguish HIV-1 Replication. J Virol. 2016;90:4681–95. [PubMed: 26912618]

[19]. Harris RS, Dudley JP. APOBECs and virus restriction. Virology. 2015;479-480:131–45. [PubMed: 25818029]

[20]. Holtz CM, Sadler HA, Mansky LM. APOBEC3G cytosine deamination hotspots are defined by both sequence context and single-stranded DNA secondary structure. Nucleic Acids Res. 2013;41:6139–48. [PubMed: 23620282]

[21]. McDaniel YZ, Wang D, Love RP, Adolph MB, Mohammadzadeh N, Chelico L, et al. Deamination hotspots among APOBEC3 family members are defined by both target site sequence context and ssDNA secondary structure. Nucleic Acids Res. 2020;48:1353–71. [PubMed: 31943071]

[22]. Desimmie BA, Delviks-Frankenberrry KA, Burdick RC, Qi D, Izumi T, Pathak VK. Multiple APOBEC3 restriction factors for HIV-1 and one Vif to rule them all. J Mol Biol. 2014;426:1220–45. [PubMed: 24189052]

[23]. Sadler HA, Stenglein MD, Harris RS, Mansky LM. APOBEC3G contributes to HIV-1 variation through sublethal mutagenesis. J Virol. 2010;84:7396–404. [PubMed: 20463080]

[24]. Alteri C, Surdo M, Bellocchi MC, Saccomandi P, Continenza F, Armenia D, et al. Incomplete APOBEC3G/F Neutralization by HIV-1 Vif Mutants Facilitates the Genetic Evolution from CCR5 to CXCR4 Usage. Antimicrob Agents Chemother. 2015;59:4870–81. [PubMed: 26055363]

[25]. Squires KD, Monajemi M, Woodworth CF, Grant MD, Larijani M. Impact of APOBEC Mutations on CD8+ T Cell Recognition of HIV Epitopes Varies Depending on the Restricting HLA. J Acquir Immune Defic Syndr. 2015;70:172–8. [PubMed: 26035050]

[26]. Monajemi M, Woodworth CF, Zipperlen K, Gallant M, Grant MD, Larijani M. Positioning of APOBEC3G/F mutational hotspots in the human immunodeficiency virus genome favors reduced recognition by CD8+ T cells. PLoS One. 2014;9:e93428. [PubMed: 24722422]

[27]. Neogi U, Shet A, Sahoo PN, Bontell I, Ekstrand ML, Banerjea AC, et al. Human APOBEC3G-mediated hypermutation is associated with antiretroviral therapy failure in HIV-1 subtype C-infected individuals. J Int AIDS Soc. 2013;16:18472. [PubMed: 23443042]

[28]. Wiegand HL, Doehle BP, Bogerd HP, Cullen BR. A second human antiretroviral factor, APOBEC3F, is suppressed by the HIV-1 and HIV-2 Vif proteins. EMBO J. 2004;23:2451–8. [PubMed: 15152192]

[29]. Smith JL, Izumi T, Borbet TC, Hagedorn AN, Pathak VK. HIV-1 and HIV-2 Vif interact with human APOBEC3 proteins using completely different determinants. J Virol. 2014;88:9893–908. [PubMed: 24942576]

[30]. Ribeiro AC, Maia e Silva A, Santa-Marta M, Pombo A, Moniz-Pereira J, Goncalves J, et al. Functional analysis of Vif protein shows less restriction of human immunodeficiency virus type 2 by APOBEC3G. J Virol. 2005;79:823–33. [PubMed: 15613310]

[31]. Duggal NK, Malik hS, Emerman M. The breadth of antiviral activity of Apobec3DE in chimpanzees has been driven by positive selection. J Virol. 2011;85:11361–71. [PubMed: 21835794]

[32]. Rawson JM, Clouser CL, Mansky LM. Rapid Determination of HIV-1 Mutant Frequencies and Mutation Spectra Using an mCherry/EGFP Dual-Reporter Viral Vector. Methods Mol Biol. 2016;1354:71–88. [PubMed: 26714706]

[33]. Apolonia L, Schulz R, Curk T, Rocha P, Swanson CM, Schaller T, et al. Promiscuous RNA binding ensures effective encapsidation of APOBEC3 proteins by HIV-1. PLoS Pathog. 2015;11:e1004609. [PubMed: 25590131]

[34]. Schneider CA, Rasband WS, Eliceiri KW. NIH Image to ImageJ: 25 years of image analysis. Nat Methods. 2012;9:671–5. [PubMed: 22930834]

[35]. Schindelin J, Arganda-Carreras I, Frise E, Kaynig V, Longair M, Pietzsch T, et al. Fiji: an open-source platform for biological-image analysis. Nat Methods. 2012;9:676–82. [PubMed: 22743772]

[36]. Li MM, Emerman M. Polymorphism in human APOBEC3H affects a phenotype dominant for subcellular localization and antiviral activity. J Virol. 2011;85:8197–207. [PubMed: 21653666]

[37]. Feng Y, Love RP, Ara A, Baig TT, Adolph MB, Chelico L. Natural Polymorphisms and Oligomerization of Human APOBEC3H Contribute to Single-stranded DNA Scanning Ability. J Biol Chem. 2015;290:27188–203. [PubMed: 26396192]

[38]. Zhen A, Du J, Zhou X, Xiong Y, Yu XF. Reduced APOBEC3H variant anti-viral activities are associated with altered RNA binding activities. PLoS One. 2012;7:e38771. [PubMed: 22859935]

[39]. Duggal NK, Fu W, Akey JM, Emerman M. Identification and antiviral activity of common polymorphisms in the APOBEC3 locus in human populations. Virology. 2013;443:329–37. [PubMed: 23755966]

[40]. Esu-Williams E, Mulanga-Kabeya C, Takena H, Zwandor A, Aminu K, Adamu I, et al. Seroprevalence of HIV-1, HIV-2, and HIV-1 group O in Nigeria: evidence for a growing increase of HIV infection. J Acquir Immune Defic Syndr Hum Retrovirol. 1997;16:204–10. [PubMed: 9390573]

[41]. Zeh C, Pieniazek D, Agwale SM, Robbins KE, Odama L, Sani-Gwarzo N, et al. Nigerian HIV type 2 subtype A and B from heterotypic HIV type 1 and HIV type 2 or monotypic HIV type 2 infections. AIDS Res Hum Retroviruses. 2005;21:17–27. [PubMed: 15665641]

[42]. Kieffer TL, Kwon P, Nettles RE, Han Y, Ray SC, Siliciano RF. G-->A hypermutation in protease and reverse transcriptase regions of human immunodeficiency virus type 1 residing in resting CD4+ T cells in vivo. J Virol. 2005;79:1975–80. [PubMed: 15650227]

[43]. Gandhi SK, Siliciano JD, Bailey JR, Siliciano RF, Blankson JN. Role of APOBEC3G/F-mediated hypermutation in the control of human immunodeficiency virus type 1 in elite suppressors. J Virol. 2008;82:3125–30. [PubMed: 18077705]

[44]. Land AM, Ball TB, Luo M, Pilon R, Sandstrom P, Embree JE, et al. Human immunodeficiency virus (HIV) type 1 proviral hypermutation correlates with CD4 count in HIV-infected women from Kenya. J Virol. 2008;82:8172–82. [PubMed: 18550667]

[45]. Ulenga NK, Sarr AD, Hamel D, Sankale JL, Mboup S, Kanki PJ. The level of APOBEC3G (hA3G)-related G-to-A mutations does not correlate with viral load in HIV type 1-infected individuals. AIDS Res Hum Retroviruses. 2008;24:1285–90. [PubMed: 18851679]

[46]. Piantadosi A, Humes D, Chohan B, McClelland RS, Overbaugh J. Analysis of the percentage of human immunodeficiency virus type 1 sequences that are hypermutated and markers of disease progression in a longitudinal cohort, including one individual with a partially defective Vif. J Virol. 2009;83:7805–14. [PubMed: 19494014]

[47]. Holtz CM, Mansky LM. Variation of HIV-1 mutation spectra among cell types. J Virol. 2013;87:5296–9. [PubMed: 23449788]

[48]. Okada A, Iwatani Y. APOBEC3G-Mediated G-to-A Hypermutation of the HIV-1 Genome: The Missing Link in Antiviral Molecular Mechanisms. Front Microbiol. 2016;7:2027. [PubMed: 28066353]

[49]. Iwatani Y, Chan DS, Wang F, Maynard KS, Sugiura W, Gronenborn AM, et al. Deaminase-independent inhibition of HIV-1 reverse transcription by APOBEC3G. Nucleic Acids Res. 2007;35:7096–108. [PubMed: 17942420]

[50]. Bishop KN, Verma M, Kim EY, Wolinsky SM, Malim MH. APOBEC3G inhibits elongation of HIV-1 reverse transcripts. PLoS Pathog. 2008;4:e1000231. [PubMed: 19057663]

[51]. Adolph MB, Webb J, Chelico L. Retroviral restriction factor APOBEC3G delays the initiation of DNA synthesis by HIV-1 reverse transcriptase. PLoS One. 2013;8:e64196. [PubMed: 23717565]

[52]. Belanger K, Savoie M, Rosales Gerpe MC, Couture JF, Langlois MA. Binding of RNA by APOBEC3G controls deamination-independent restriction of retroviruses. Nucleic Acids Res. 2013;41:7438–52. [PubMed: 23761443]

[53]. Stavrou S, Crawford D, Blouch K, Browne EP, Kohli RM, Ross SR. Different modes of retrovirus restriction by human APOBEC3A and APOBEC3G in vivo. PLoS Pathog. 2014;10:e1004145. [PubMed: 24851906]

[54]. Albin JS, Brown WL, Harris RS. Catalytic activity of APOBEC3F is required for efficient restriction of Vif-deficient human immunodeficiency virus. Virology. 2014;450-451:49–54. [PubMed: 24503066]

[55]. Gillick K, Pollpeter D, Phalora P, Kim EY, Wolinsky SM, Malim MH. Suppression of HIV-1 infection by APOBEC3 proteins in primary human CD4(+) T cells is associated with inhibition of processive reverse transcription as well as excessive cytidine deamination. J Virol. 2013;87:1508–17. [PubMed: 23152537]

[56]. Refsland EW, Stenglein MD, Shindo K, Albin JS, Brown WL, Harris RS. Quantitative profiling of the full APOBEC3 mRNA repertoire in lymphocytes and tissues: implications for HIV-1 restriction. Nucleic Acids Res. 2010;38:4274–84. [PubMed: 20308164]

[57]. Holmes M, Zhang F, Bieniasz PD. Single-Cell and Single-Cycle Analysis of HIV-1 Replication. PLoS Pathog. 2015;11:e1004961. [PubMed: 26086614]

[58]. Rawson JM, Heineman RH, Beach LB, Martin JL, Schnettler EK, Dapp MJ, et al. 5,6-Dihydro-5-aza-2'-deoxycytidine potentiates the anti-HIV-1 activity of ribonucleotide reductase inhibitors. Bioorg Med Chem. 2013;21:7222–8. [PubMed: 24120088]

[59]. Beach LB, Rawson JM, Kim B, Patterson SE, Mansky LM. Novel inhibitors of human immunodeficiency virus type 2 infectivity. J Gen Virol. 2014;95:2778–83. [PubMed: 25103850]

[60]. Harrington RD, Geballe AP. Cofactor requirement for human immunodeficiency virus type 1 entry into a CD4-expressing human cell line. J Virol. 1993;67:5939–47. [PubMed: 7690415]

[61]. Vodicka MA, Goh WC, Wu LI, Rogel ME, Bartz SR, Schweickart VL, et al. Indicator cell lines for detection of primary strains of human and simian immunodeficiency viruses. Virology. 1997;233:193–8. [PubMed: 9201229]

[62]. Gervaix A, West D, Leoni LM, Richman DD, Wong-Staal F, Corbeil J. A new reporter cell line to monitor HIV infection and drug susceptibility in vitro. Proc Natl Acad Sci U S A. 1997;94:4653–8. [PubMed: 9114046]

[63]. Victoria JG, Lee DJ, McDougall BR, Robinson WE Jr. Replication kinetics for divergent type 1 human immunodeficiency viruses using quantitative SYBR green I real-time polymerase chain reaction. AIDS Res Hum Retroviruses. 2003;19:865–74. [PubMed: 14585218]

Highlights

- G-to-A mutations, characteristic of A3 editing, are rare during HIV-2 replication
- A3F, A3G, and A3H restrict HIV-2 infection in the absence of Vif, but not A3D.
- A3F and A3G act as mutagens, while A3H blocks reverse transcription.
- This study is the first comprehensive assessment of A3 activity against HIV-2.

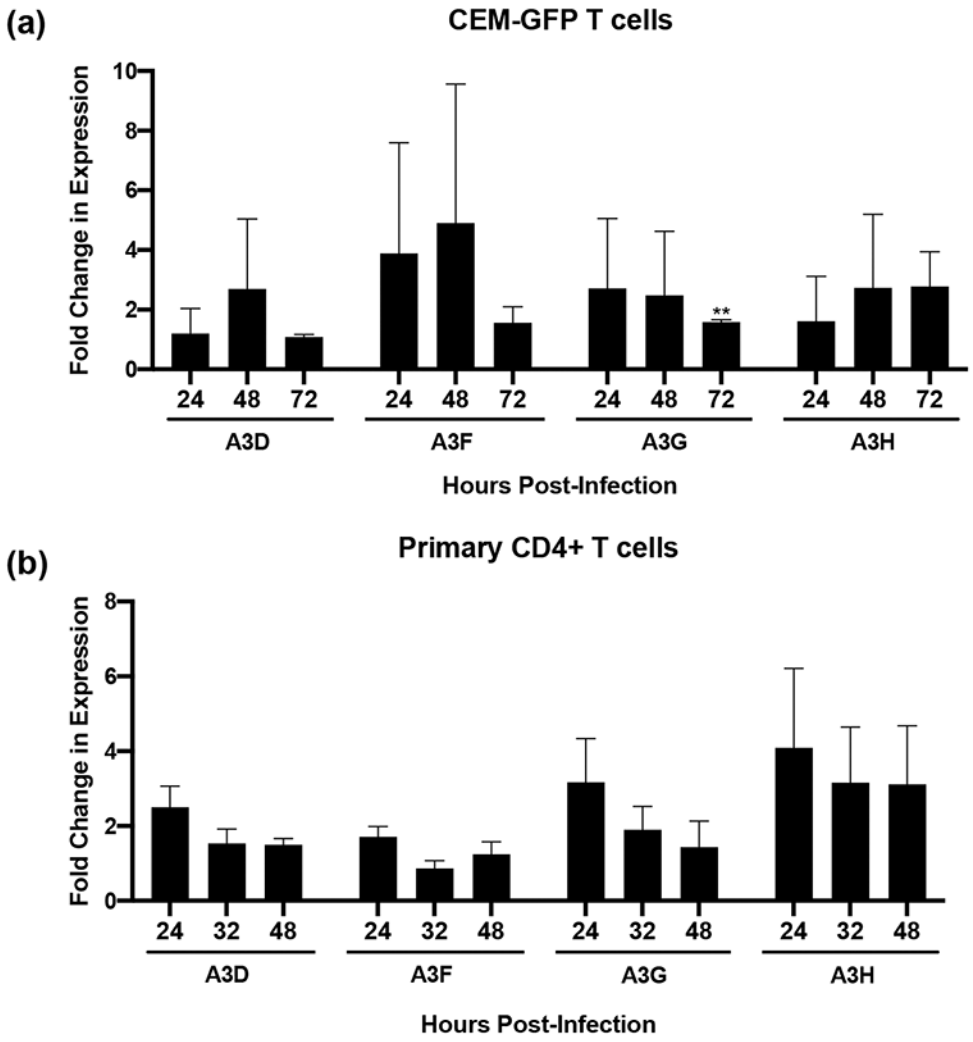

Figure 1. HIV-2 infection does not robustly stimulate A3 expression in a T cell line and human primary T cells.

The fold change in *A3* mRNA levels was quantified by RT-qPCR following infection with the HIV-2 vector virus HIV-2 pROD-10 MIG in (A) CEM-GFP cells, and (B) primary human CD4+ T cells isolated from whole blood of 3 separate donors. Expression of *A3G* was significantly increased (1.5-fold; $^{**}P=0.002$) at 72 h in CEM-GFP cells. In both T cell types, expression of all genes peaked at or prior to 48 h. Results shown represent the mean and standard error of mean of 3 independent replicates performed in technical duplicate.

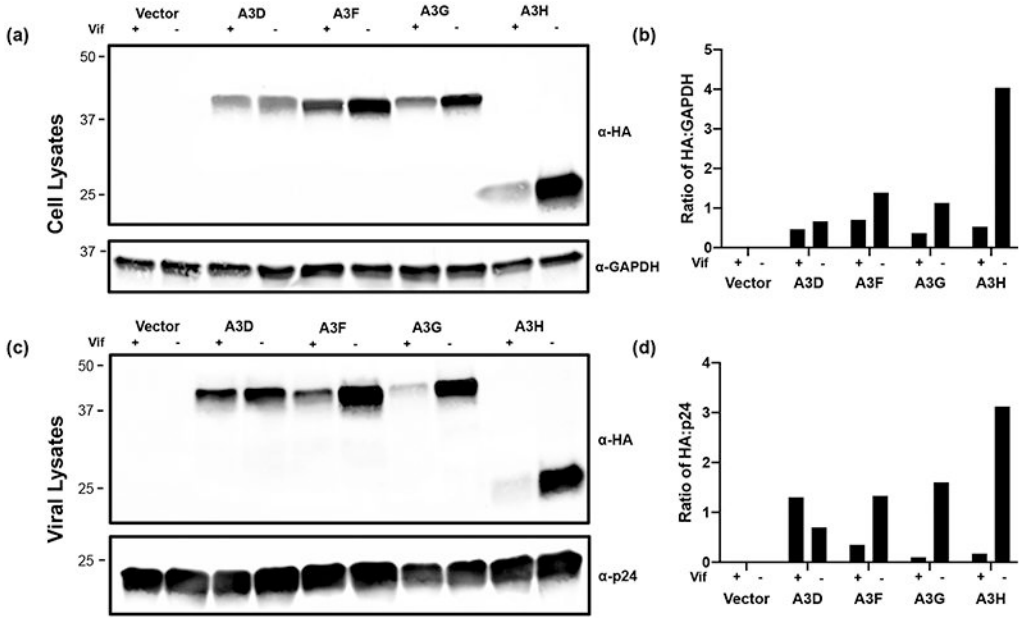

Figure 2. Virion incorporation of A3F, A3G, and A3H is inhibited by HIV-2 Vif.

Immunoblot analysis was conducted to determine the relative amount of HA-tagged A3 protein levels in the presence or absence of HIV-2 Vif. A representative immunoblot from (A) producer cell lysates and (B) its corresponding quantification are shown. A3 protein was detected using an anti-HA antibody and were standardized to the cellular loading control, GAPDH, using densitometry analysis. A representative immunoblot from (C) viral lysates and (D) its corresponding quantification are shown. Levels of A3 proteins in viral lysates were standardized to the viral loading control, Gag, which was detected using an anti-p24 antibody that cross-reacts with HIV-2. The representative blots shown were selected from 4 independent replicates.

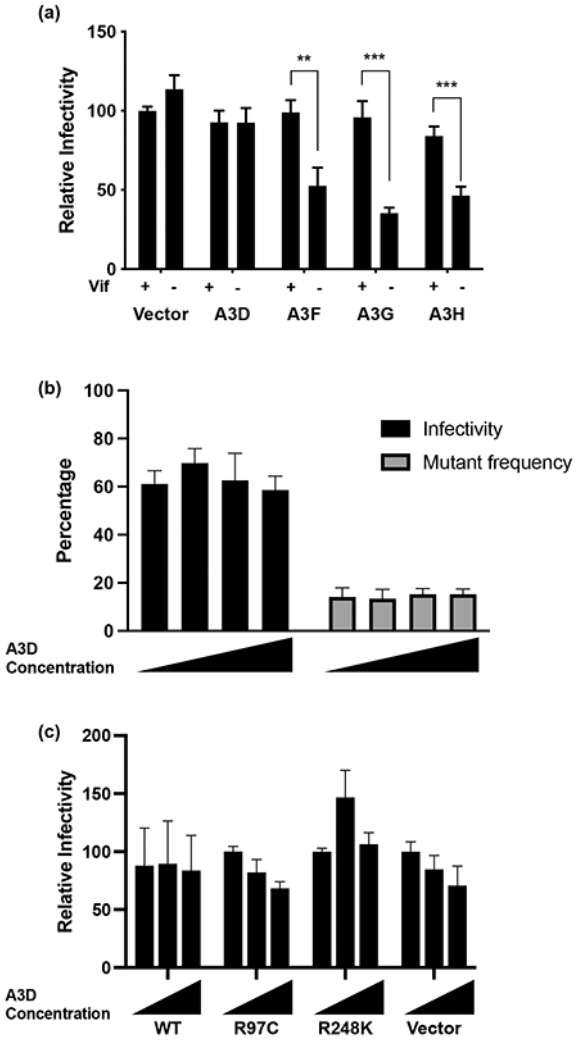

Figure 3. A3F, A3G, and A3H restrict HIV-2 infectivity, but not A3D.

(A) Relative infectivity analysis. Flow cytometry was used to assess the relative percent infectivity of Vif+ and Vif− HIV-2 pROD10-MIG vector virus. Rates of infection were normalized to the rate of infection for the Vif+ virus produced in the presence of the empty vector control. A3F, A3G, and A3H significantly reduced the infectivity of the virus in the absence of Vif (**P <0.01, ***P <0.001). (B) Titration of A3D expression in virus-producer cells. Infectivity of HIV-2 (black bars) and the frequency of mutants in the population (gray bars) are indicated. (C) Analysis of A3D haplotypes on HIV-2 restriction. The relative infectivity of Vif− HIV-2 pROD-10 MIG vector virus was analyzed in the presence of WT A3D, R97C A3D, and R248K A3D mutants, over a range of concentrations, compared with the empty vector control. Results shown represent the mean and standard deviation of 3 independent replicates completed in technical duplicate.

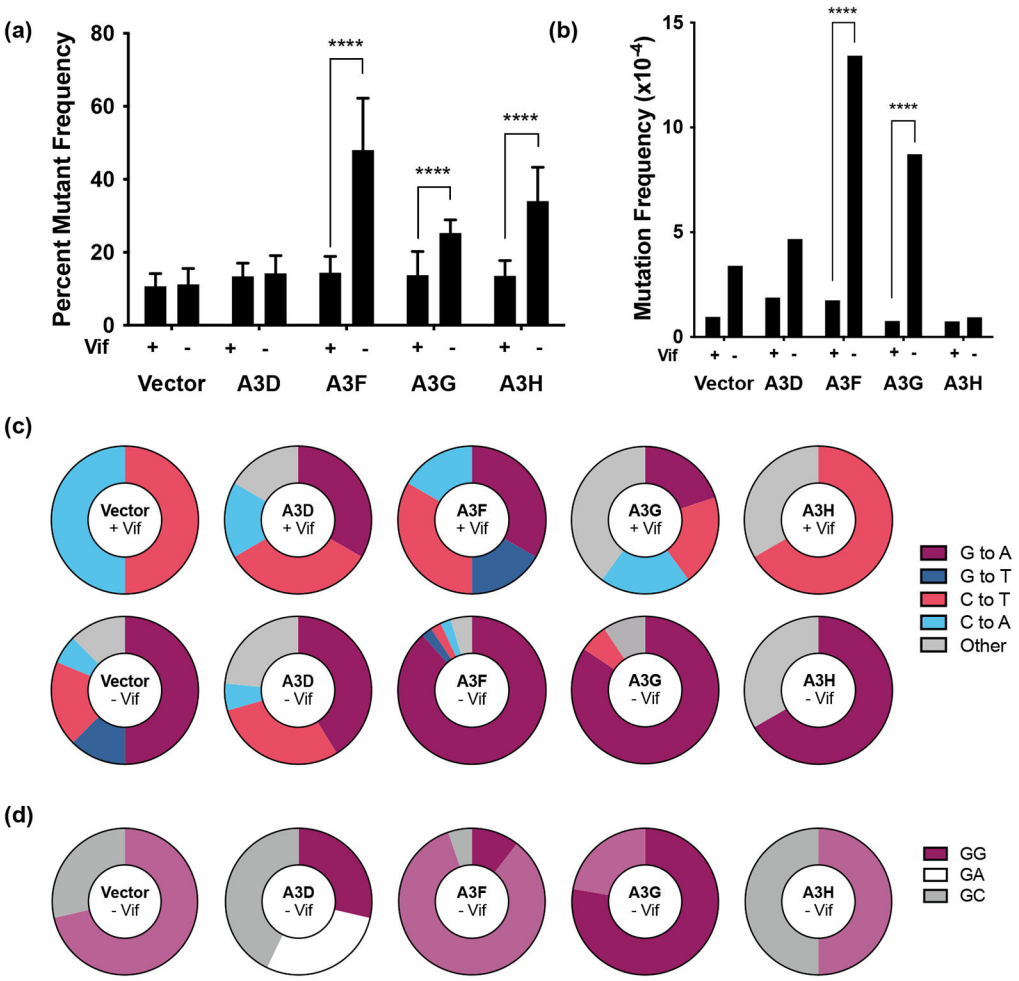

Figure 4. A3F, A3G, and A3H increase the HIV-2 mutant frequency of HIV-2 mutants and increase the frequency of G-to-A transition mutations.

(A) Relative mutant frequency analysis. The relative frequency of mutants in the populations of HIV-2 pROD-10 MIG vector virus-infected cells was assessed using flow cytometry. Mutant frequency was significantly increased by A3F, A3G, and A3H in the Vif− virus relative to the Vif+ virus (**** P <0.0001). (B) Sequencing of HIV-2 proviruses. Sanger sequencing of *EGFP* in HIV-2 pROD-10 MIG proviruses isolated from U373-MAGI-CXCR4 gDNA was used to quantify the mutagenic capacity of A3D, A3F, A3G, and A3H. A3F and A3G increased the mutation frequency of Vif− HIV-2 approximately 7-fold and 11-fold compared with the Vif+ virus, respectively (**** P <0.0001). (C) HIV-2 mutation spectra analysis. Shown are pie charts indicating the spectra of mutations observed in HIV-2 proviruses with expression of A3D, A3F, A3G, and A3H in the presence and absence of Vif expression. (D) Dinucleotide context of G-to-A mutations observed within Vif− HIV-2.

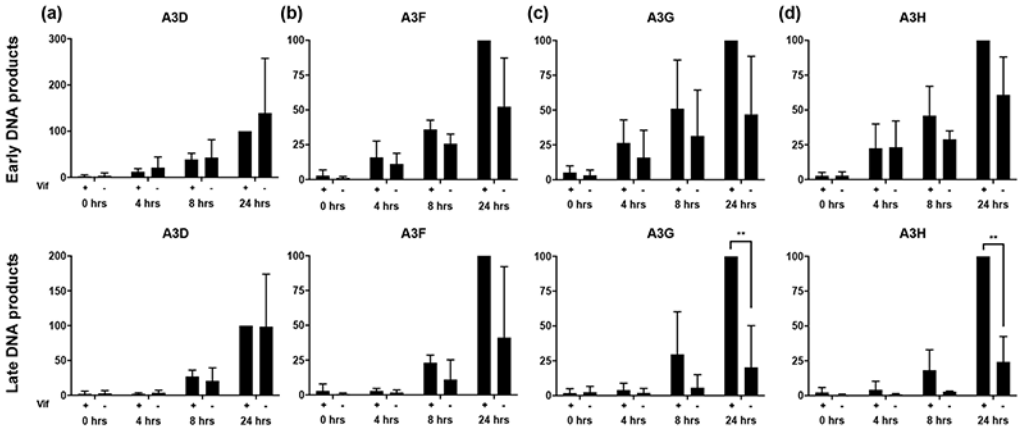

Figure 5. A3G and A3H inhibit the accumulation of reverse transcription DNA products at late stages of HIV-2 infection.

Accumulation of reverse transcription products associated with (A) A3D, (B) A3F, (C) A3G, and (D) A3H expression was measured using qPCR and was normalized to the quantity of product measured at 24 h with the Vif+ virus. DNA products at early and late stages of reverse transcription were measured over 24 hours. Late-stage replication was inhibited by A3G and A3H (** P <0.01).

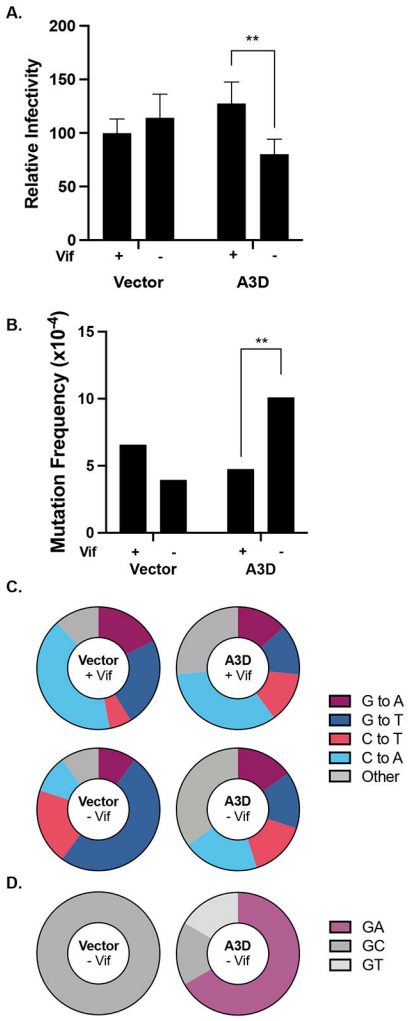

Figure 6. Concomitant reduction in infectivity and increased mutation frequency of Vif− HIV-1 by A3D.

(A) Relative infectivity analysis. Flow cytometry was used to assess the relative percent infectivity of Vif+ and Vif− HIV-1 MIG vector virus. Rates of infection were normalized to the rate of infection for the Vif+ virus produced in the presence of the empty vector control. A3D significantly reduced the infectivity of the virus in the absence of Vif (**P <0.01). (B) Sequencing of HIV-1 proviruses. Sanger sequencing of *EGFP* in HIV-1 MIG proviruses isolated from U373-MAGI-CXCR4 gDNA was used to quantify A3D mutagenic capacity. A3D increased the mutation frequency of Vif− HIV-1 approximately 2-fold compared with the Vif+ virus (**P <0.01). (C) HIV-2 mutation spectra analysis. Shown are pie charts indicating the spectra of mutations observed in HIV-1 proviruses with expression of A3D in the presence and absence of Vif expression. (D) Dinucleotide context of G-to-A mutations observed within Vif− HIV-1.

Table 1.

Mutational analysis of *EGFP* in recovered HIV-2 proviruses.

A3 Protein	Vif	Base Pairs Sequenced	Colonies Sequenced	Mutations Observed	Mutation Frequency (mut/bp)	Hypermutants[a]
Vector	+	41,585	57	4	9.6×10^{-5}	−
	−	44,083	60	15	3.4×10^{-4}	−
A3D	+	31,848	46	6	1.88×10^{-4}	−
	−	36,342	54	17	4.68×10^{-4}	−
A3F	+	32,025	49	6	1.75×10^{-4}	3
	−	34,217	45	43	1.34×10^{-3}	2
A3G	+	51,750	67	4	7.7×10^{-5}	−
	−	36,629	51	32	8.73×10^{-4}	1
A3H	+	39,956	57	3	7.5×10^{-5}	−
	−	31,926	45	3	9.4×10^{-5}	−

[a]Hypermutants were defined as proviruses with >1 mutation per 100 base pairs sequenced.

Table 2.

Summary of anti-HIV-2 activity of A3D, A3F, A3G, and A3H.

A3 Protein	Restricts Infectivity[a]	Enacts Mutagenesis[a,b]	Inhibits Reverse Transcription[a]
A3D	−	−/−	−
A3F	+	+/+	−
A3G	+	+/+	+
A3H	+	−/+	+

[a] +, yes; −, no

[b] +/+, increases the proviral mutation frequency and the proportion of functional mutants; −,+ does not increase the proviral mutation frequency but does increase the proportion of functional mutants